

A Modular Approach to Soft Robots

Cagdas D. Onal and Daniela Rus

Abstract—This paper describes a modular approach to creating soft robotic systems. The basis of these systems is an elastomeric actuation element powered by direct mechanical energy in the form of pressurized fluids. Fluidic elastomer actuators are fast and inexpensive to fabricate and offer safety and adaptability to robotic systems. Arrangements of these units can yield arbitrarily complex motions and achieve various functionalities. Actuation power can be generated on-board by a pneumatic battery, which harnesses the catalyzed chemical decomposition of hydrogen peroxide into oxygen gas, for mobile implementations. The modular nature of these robots enable distributed sensing and computation elements. Composition techniques of such soft robots are defined. Example systems are demonstrated and analyzed.

I. INTRODUCTION

This paper discusses a new approach to creating soft and compliant robots, relying on a novel actuator technology. These actuators, tagged as fluidic elastomer actuators (FEAs) [1], [2], [3] comprise synthetic elastomer films as pneumatic or hydraulic deformation elements fabricated by molding. They are operated by the expansion of embedded fluidic channels under pressure input [4]. FEAs have a large actuation range, limited only by the material's mechanical strength. They are modular (Figs. 1, 2), such that actuation units can be composed in various, possibly redundant arrangements to achieve exceedingly complex motions. This way, an intrinsically safe and adaptable actuation system can be distributed over the body in series, parallel, or a combination of the two architectures. Potential applications of this family of soft robots include human interaction and assistance, wearable tactile interfaces, artificial muscles, and active orthoses.

Robots are creeping into our daily lives at an increasing rate and making positive changes. It is important to investigate the compatibility of robotic architectures to human-occupied unstructured and dynamic workspaces. Robots are traditionally rigid machines, designed to perform a small set of tasks efficiently, often with limited adaptability. Built of rigid links and joints, they are unsafe to interact with for human beings, which leads to the separation of human and robotic workspaces in factories. Adaptation in robotic operation is typically achieved by the software layer, which adds a burden on control systems and planners. On the other hand, hardware remains a bottleneck in developing new

This work was supported by the Boeing Company, National Science Foundation (NSF) Expeditions Program CCF 1138967 (Printable Programmable Machines) and Emerging Frontiers in Research and Innovation (EFRI). We are grateful for this support.

C. D. Onal and D. Rus are with the Computer Science and Artificial Intelligence Laboratory, Massachusetts Institute of Technology, Cambridge, MA 02139, USA {cagdas, rus}@csail.mit.edu

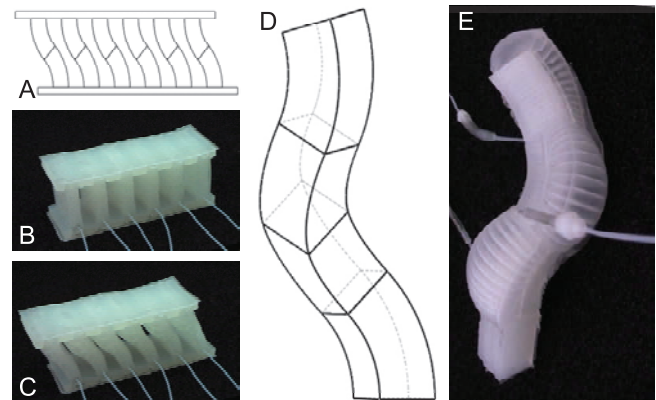


Fig. 1. Example fluidic soft actuators that demonstrate the range of functionalities achievable by composing FEA modules in different arrangements. (A-C) A soft linear positioner made of a hybrid composition of twelve FEA modules. Each finger comprises two FEAs attached in series, bending in opposite directions to achieve linear motion. Fingers are connected in parallel. (D-E) A soft kinematic chain made of four bidirectional fluidic elastomer bending actuators arranged in series. The modules are composed to bend in alternating directions to achieve a soft 3-D manipulator arm.

functionalities as it is generally more expensive and takes longer to update.

One solution we propose to these problems is to incorporate flexibility to robotic bodies. Given their small minimum stiffness, soft actuators are safe, as they can deform and take in much of the energy in case of a crash [5]. This will open the door for applications where robots work with humans in factories, in the field, or at home. A compliant structure brings many benefits to robots; environmental uncertainty is less of a problem and goals can be achieved without complex modeling and planning requirements. In one aspect, a soft robot takes some of these requirements off the software system by embedding intelligence in the mechanics of its body in the form of inherent safety and adaptability. Application areas of practical soft robotic mechanisms include artificial muscles [6], medical robotics, bio-inspired robotics, conformal grippers for pose-invariant and shape-invariant grasping, and human interaction or human assistive technologies.

On the other hand, this family of soft robots has its own unique set of practical and theoretical challenges. First, having a fluidic actuation principle requires a pressure source [7], which should also be portable for mobile applications. Second, additional valving hardware is necessary to address and drive individual actuators. Third, models to describe the behavior of the elastomeric materials or the operation of the systems are typically complicated or non-existent.

We address these challenges as follows. To provide the necessary mechanical energy for actuation, we develop a

chemical pressure generator called the pneumatic battery [2]. This is a new portable power source that enables tetherless mobile applications of soft robots. To drive the FEAs, we utilize custom [3] or commercial valves operated by a computation system, handled by custom PCBs. Small sensors can be distributed over the body to provide feedback for computation. Finally, we characterize the actuators and develop physical, or empirical models to describe their behavior, as well as forward and inverse kinematic models of soft linkages as a step towards soft manipulators.

Soft robotic literature is blossoming with many interesting works focusing on building functional soft actuators and systems. A miniature 3-D pneumatic rubber actuator is described in [8]. This actuator has a cylindrical outer shell, and a segmented inner shell to achieve bending and axial deformations. Another interesting rubber actuator has a pleated structure [9], which can generate rotary motion. It was developed for rehabilitation applications and designed to replace conventional linear pneumatic actuators.

A recent work [10] describes a bio-inspired robotic platform based on an octopus arm. The arm is made of silicone rubber and driven with embedded tendons. It can locomote by pushing, and grasp objects similar to its biological counterpart.

In previous work, we have discussed the development of some of the mechanisms that make up our soft robots. In [1], we focused on a specific mobile robot and described the fabrication and control of it. In [2] we improved upon our static model of FEAs and discussed the pneumatic battery. In [3], we showed that we can build low-cost, embeddable, and energy-efficient valves to drive our actuators. In this paper, we describe our approach to building soft robots at a system-level with examples, based on the results of previous research. We achieve this by distributed arrangements of FEAs in arbitrary 3-D shapes.

The contributions of this work are as follows:

- Description and analysis of key underlying technologies that make up our fluidic elastomer soft robots.
- Composition techniques of FEA modules for soft robotics.
- Examples of several soft robotic platforms fabricated in various compositions.

II. SOFT ROBOT ARCHITECTURE

The general architecture we developed for fluidic soft robots can be described by a sketch as shown in Fig. 3. As seen in this figure, a soft robot has all the sub-systems of a conventional robot. It has four main components; an actuation system, a perception system, driving electronics, and a computation system, with corresponding power sources. The key difference is the separation of the actuation power from the rest of the system, using mechanical energy in the form of pressure instead of electrical energy. Since FEAs are directly powered by pressure, no energy conversion takes place at the actuators. Since electrical signals are the language of computation, additional valving hardware is also

incorporated into the architecture to electrically address and isolate the mechanical actuation system.

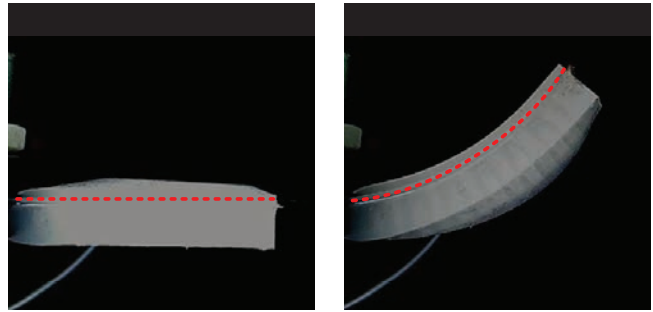


Fig. 2. A fluidic elastomer bending actuator with large actuation range. The actuator in the initial state is shown on the left. As a constant pressure of 20.7 kPa is applied, embedded channels expand laterally and bend the composite due to an inextensible thin sheet on the top layer, indicated by a dashed red curve, on the right. Upon removal of pressure, the initial configuration is restored.

FEAs are at the core of our soft robots. They are essentially fluidic expansion modules, constrained in order to generate an out-of-plane bending deformation. They accomplish this using a bimorph structure of two layers, such that the pressure input expands fluidic channels, which are embedded in the first layer, in the long axis of the actuator and the second layer constraints the axial tension of the elastomer to induce bending. This behavior is experimentally shown in Fig. 2, where a red dashed curve is augmented to indicate the extension constraint in the second layer. Displacement requirements are satisfied in the design phase by the geometry and number of elements that constitute the actuator.

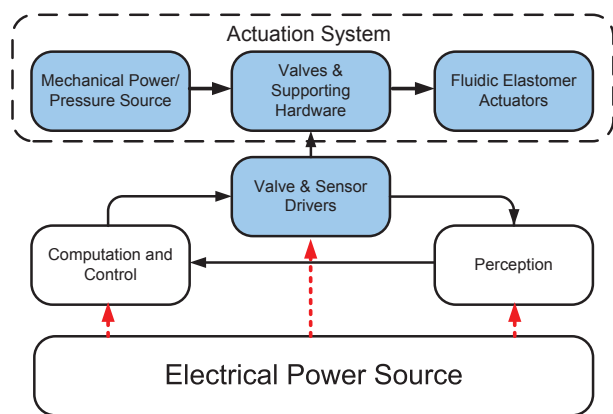


Fig. 3. The architecture of a soft robot using fluiding actuation. Components unique to fluidic soft robots are shaded in blue.

A. Fabrication

As shown in Fig. 4, the fabrication procedure of the actuators starts by molding both layers separately out of a very soft silicone rubber material (Smooth-on™ Ecoflex™ Supersoft 0030). The molds are created by a fused deposition modeling (3-D printing) process on ABS plastic. The first

mold carries the negative of parallel rectangular fluidic channels connected on both ends in a serpentine arrangement. The second mold has a thin rectangular opening, with the same length and width as the first layer. In this mold, an inextensible flexible material, namely a fabric sheet is placed before silicone rubber is poured. After curing, both layers are demolded and the first layer is dipped on a thin layer of uncured elastomer of the same material. Finally, the two layers are brought into conformal contact and cured together.

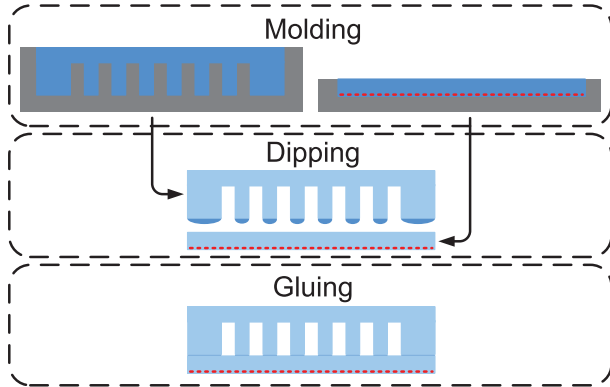


Fig. 4. Fabrication procedure of fluidic elastomer actuator modules. Silicone rubber elastomers are molded in two layers. First layer on the left creates continuous fluidic channels and the second layer embeds the inextensible constraint layer (red dashed line). The first layer is dipped onto a thin layer of uncured elastomer after demolding and placed on top of the second layer to seal the fluidic channels off. The darker blue color indicates uncured polymer.

B. Actuation

In [2], we have derived a physical static model of out-of-plane displacement for bending-type FEAs. This model relates the pressure input to output displacement, using the geometric and material properties of the actuators and is very useful for designing FEAs for different requirements. For realistic position control applications, however, a dynamic model of displacement is more useful. This has two reasons. First, a static model is only relevant for long time scales or low frequencies. Second, and more importantly, it is impractical to change the pressure input for individual actuators. Instead, utilizing the dynamics of motion by switching valves on and off to converge to a target displacement is more appropriate.

Fortunately, fluidic tubing and channels act as impedances and fluidic chambers act as capacitances in a circuit equivalent, which enables a second-order differential equation to fundamentally describe the motion dynamics of FEAs as seen in Fig. 5. This figure displays experimental data of out-of-plane displacement, using external image processing of a calibrated camera feed of a FEA clamped on one end, as a function of time for a constant inlet pressure of $P_{in} = 20.7$ kPa. A solution to the second-order ordinary differential equation given as

$$\delta = C_o + C_1 \exp(-t/\tau_1) + C_2 \exp(-t/\tau_2), \quad (1)$$

TABLE I
DYNAMIC PARAMETERS OF A SAMPLE FLUIDIC ELASTOMER ACTUATOR.

| P_{in} | τ_{on} | τ_{off} | δ_{max} |
|----------|-------------|--------------|----------------|
| 20.7 kPa | 1.44 sec | 0.36 sec | 11.54 mm |

where δ is the out-of-plane displacement of the actuator, $C_i, i \in [0, 2]$ are constant coefficients, and $\tau_k, k \in 1, 2$ are the dynamic time constants. This overdamped solution is fitted to both on and off states of the valve separately, since the time constants of these states may vary based on the flow paths of air for inflation and venting actions. For this case, the primary time constants for both cases are tabulated in Table I as well as other parameters for reference. Note that, the maximum displacement (δ_{max}) in this table is analytically predicted by the static model in [2] yielding a complete dynamic model based on a given pressure input P_{in} .

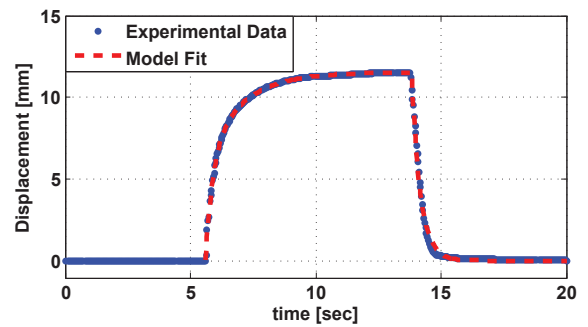


Fig. 5. Experimental data of out-of-plane displacement of a fluidic elastomer actuator with respect to time. Separate second-order differential equations are fitted to the actuation and venting phases. This model provides accurate representation of the motion dynamics.

C. On-board Power

The second big challenge for pressure-operated soft robots is the power source for actuation. Current off-the-shelf pressure sources are generally limited to compressors or pumps and compressed air cylinders. If we draw an electrical analogy, compressors are similar to generators as they essentially convert electrical energy into mechanical energy by a periodic motion, and cylinders are similar to capacitors as they store a pressurized fluid in a certain volume and discharge upon usage. Miniature compressors use valuable electrical energy, and cylinders in useful form factors do not offer longevity. What is missing for fluidic systems is the equivalent of a battery, where a chemical reaction generates the necessary energy for actuation using a fuel.

We have developed such a device, which is a chemically operated portable pressure source we call a pneumatic battery, in [2]. The battery operates by the catalyzed decomposition of hydrogen peroxide (H_2O_2) into oxygen and water in a closed cylindrical container, with a mechanical self-regulation system to control the amount of generated pressure to remain around a certain value. This critical pressure value is a design variable and can be tuned by a set of analytical

equations of self-regulation detailed in [2]. A rotationally invariant design, and a hydrophobic filter before the outlet enable the pneumatic battery to operate in any orientation.

Recently, we made improvements to this original design. The latest pneumatic battery design is shown in Fig. 6. All of the changes over the design in [2] are on the self-regulation mechanism on the left side. We have replaced the silver catalyst with a platinum plated plastic, since silver oxidizes and gets poisoned by some of the inhibitors in the H_2O_2 solution. The geometry of the catalyst is also changed from a 2-D sheet to a 3-D hollow cylinder to increase surface area. To accommodate for the third dimension, the deflector has side walls included to properly seal around the catalyst and stop the reaction at the critical pressure value.

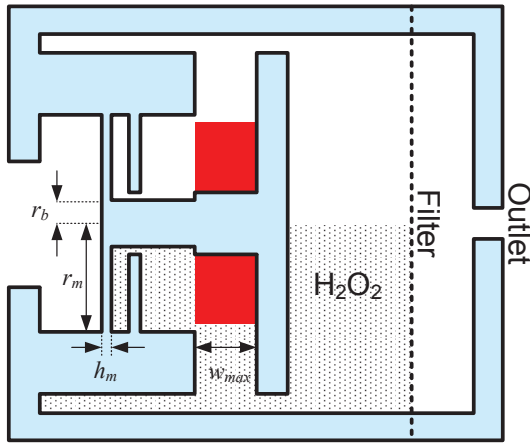


Fig. 6. Side-view sketch of the latest pneumatic battery mechanism, using hydrogen peroxide as a fuel. A deflector on the left deforms with increasing pressure and completely seals off the catalyst (red) from the solution at a tuned critical pressure, effectively stopping the gas generating reaction. The gas is filtered through a hydrophobic membrane filter with sub-micron pores on the right, before the outlet.

The air chamber on the left is also opened to atmospheric pressure, to simplify the design for self-regulation. The deflector membrane is a flat circular plate, with radius r_m and thickness h_m . For the pressure regulation to operate, this membrane needs to deflect by w_{max} at a critical gauge pressure value of P_c . Since the left side of the membrane is subject to atmospheric pressure at all times, the only equation that governs the membrane deflection is [2]

$$w(r) = \frac{\Delta P r_m^4}{64K} \left(1 - \left(\frac{r}{r_m} \right)^2 \right)^2 \quad (2)$$

in the radial axis, where $K = \frac{Eh_m^3}{12(1-\nu^2)}$ is the flexural rigidity, E is the Young's modulus, and ν is the Poisson's ratio of the plate. Solving for h_m for $w(r_b) = w_{max}$, i.e. the deflection of the plate at $r = r_b$, the radius of the protruding boss, and $\Delta P = P_c$, gives us the membrane thickness required for a given cut-off pressure value.

Using this process, we fabricated a new pneumatic battery to operate at a critical pressure value of 68.9 kPa. Experimental results are displayed in Fig. 7. A Honeywell pressure transducer is used to monitor the pressure inside the battery

during operation. We can see that the pressure quickly rises and converges to a constant value around the predicted cut-off pressure, indicated by a red dashed line. This curve also shows repeatability as the cylinder is depressurized three times and similar pressure build-up curves are achieved. Note that, while our main focus is on the passive self-regulation mechanism in these experiments, the speed of this device can also be adjusted using a higher H_2O_2 concentration and larger catalyst area.

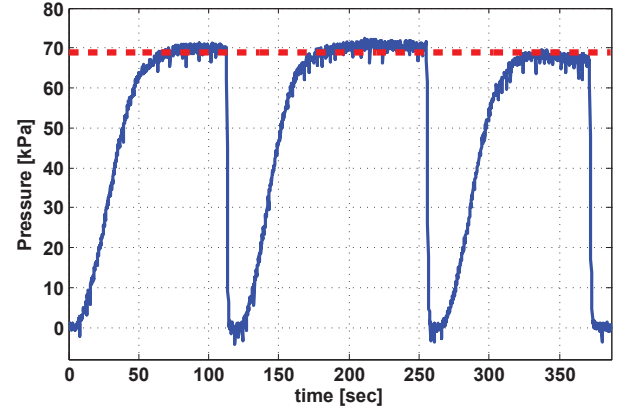


Fig. 7. Experimental results of pressure self-regulation in the pneumatic battery using a 50% wt. H_2O_2 solution in water. The reaction stops around a critical pressure value of 68.9 kPa (10 psi), based on the deflection model of the membrane under pressure. This target cut-off pressure is indicated by the red dashed line. The battery is vented three times to show repeatability.

D. Perception

For autonomous operation, a robot also needs to know or estimate its current state. This is a fundamental requirement that applies to soft robots as well. However, since compliance enables better adaptation, sensors can be simpler. For instance, we have successfully closed the loop for a rolling soft robot using only light sensitive resistors distributed over the body on each FEA module in [1]. These sensors return continuous measurements for the amount of light they see. We simplified these measurements further by thresholding to achieve logic 'up' or 'down' signals. This is enough to determine which modules are facing the ground and which are exposed to ambient light. The resulting bit array represents the state of the robot sufficiently to determine which FEA needs to be actuated to keep the body rolling forward. This exemplifies our approach to sensing for soft robots; distribution of relatively simple sensors embedded on each module to generate information on the overall state of the robot.

We are currently working on another technology compatible with FEA modules; soft curvature sensors [11], [12], [13]. These sensors generally have similar layered structures, where multiple thin layers are sandwiched and a physical property of the outer layer changes under tension caused by the overall bending of the sensor. Since FEAs need a flexible constraint on one side to generate bending, the inextensible fabric mesh can be substituted by these custom curvature

sensors without any change in the fabrication process. The resulting modules will enable distributed sensing as well as distributed actuation.

E. Computation

By virtue of increasingly cheaper and small form-factor components, computation for exceedingly complex tasks is tractable for our soft robots. The electrical hardware comprises microcontrollers (MCUs), driver circuits, and power electronics with LiPoly batteries. Using surface mount chips on flexible circuit boards enables the placement of computation in a smaller area than our current FEA modules. In [1], we used a custom flexible circuit board that houses one Atmel Atmega88PA MCU for each module in a distributed arrangement. With distributed light sensors, modules communicated with their neighbors to determine the right moment to actuate in a decentralized gait algorithm.

Flexible circuits are, again, compatible with soft modules, such that they can be attached to the inextensible side of the FEAs for operation. However, a compliant robot does not have to have a completely soft body. One example is our rolling soft mobile robot, called Flipper, which can carry the pneumatic battery at its core, shown in Fig. 10. As a consequence, this robot has a part that doesn't deform, a convenient place, where we attached a custom conventional printed circuit board (PCB) that has all the described computation sub-systems, using an Atmel Attiny13A MCU, running off of two 4.1 gr LiPoly batteries.

III. MODULAR COMPOSITION FOR SOFT ROBOT ACTUATORS

FEA modules are bending elements by themselves. By composing these basic modules in various arrangements, increasingly complex motions can be generated for soft robots with a multitude of functionalities. In this section, we describe the serial, parallel, and hybrid arrangements of soft robotic platforms with examples. The simplest arrangement is at the module level. Placing two bending actuators together in such a way that they sandwich and share a single inextensible layer yields actuators that can bend in both directions, called bidirectional FEAs.

A. Serial Composition

A serial arrangement of bidirectional FEAs bending around the same axis creates a soft kinematic chain. A similar robot was constructed in [1] to achieve inchworm-like locomotion. In contrast, in this paper the soft linkage is placed on a flat surface and the bending axis of the modules is aligned with the normal vector of the surface. This way, the robot is constrained to move in 2-D planar coordinates. The most obvious application of such a robot is a soft manipulator arm. We have previously built two instances of serial soft robots, the inchworm and a soft manipulator arm as shown in Fig. 1(D-E). This soft manipulator is a 3-D implementation, resembling an octopus arm or an elephant trunk, created by arranging bidirectional FEAs in alternating bending axes.

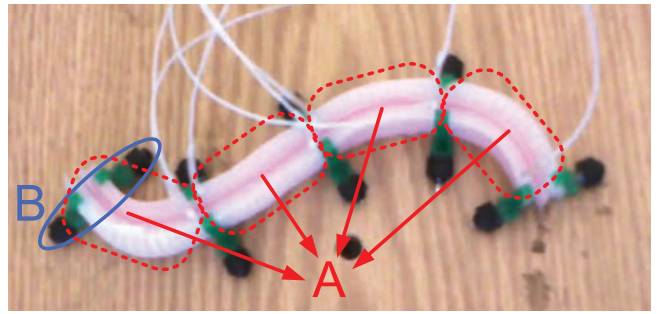


Fig. 8. Prototype of a soft snake robot, made of four bidirectional fluidic elastomer actuator segments (A) connected in series. The pink curve in the center is the inextensible layer. Directional frictional properties of snakes are generated using passive wheels attached to green holders between segments (B).

In this paper, we developed a soft robot body using serial composition; a soft snake robot shown in Fig. 8. A recent review of snake-like robots is given in [14]. Snake locomotion is well studied in the robotics community because it is an efficient form of crawling locomotion in natural environments without the complexity of limb motions [15]. Snakes achieve this by anisotropic frictional properties of their skin [16], [17]. Friction forces in the normal direction of the body axis are larger than those along the body.

This special frictional behavior in conjunction with a traveling sinusoidal wave in curvature κ along the body written as

$$\kappa(s, t) = \alpha \cos(2\pi(s + t/T)) \quad (3)$$

creates forward propulsion, where $s \in [0, 1]$ is the normalized arc length of the body neutral axis, α is the amplitude and T is the period of the wave [16].

To achieve snake-like locomotion, we built a four-segment soft kinematic chain out of bidirectional FEA modules. We attached passive wheels between segments to simulate the frictional properties of snake skin. For better visibility we used a pink inextensible layer and green laser-cut wheel holders. The resulting prototype is shown in Fig. 8. It took approximately 14 hours to build this robot.

The locomotion gait algorithm of the soft snake is based on two observations. First, input pressure directly affects the curvature of segments as it essentially generates a bending moment around the neutral axis. Second, (3) is given for a continuous system, since we have a segmented structure, we discretize this equation as

$$\kappa_i(t) = \alpha \cos(2\pi(i/n_s + t/T)), \quad (4)$$

where κ_i is the curvature of the i th segment and $n_s = 4$ is the number of segments. To approximate these curvature values we rely on the dynamics of FEAs discussed in Section II and actuate one side of the i th segment on for positive values of κ_i and the other side for $\kappa_i < 0$. By setting the actuation period sufficiently high, $T = 10$ sec determined empirically, we approximate the sinusoidal curve by a square wave smoothed by the dynamics of actuation. The amplitude of undulation is determined by the constant pressure input

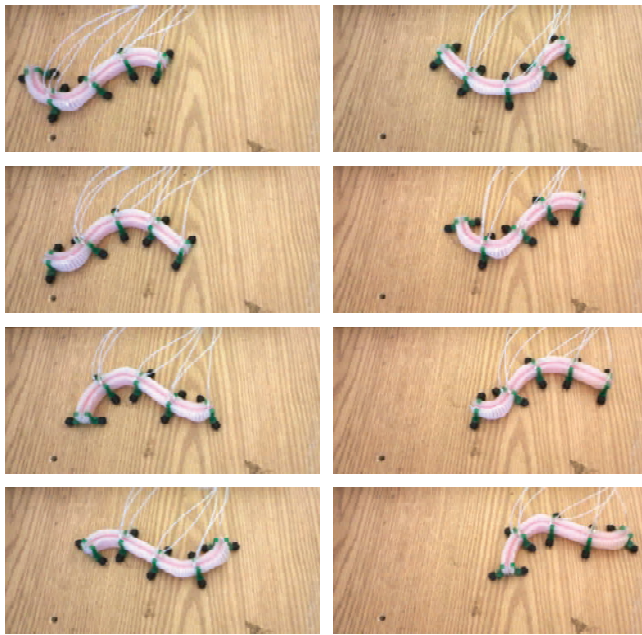


Fig. 9. Soft snake prototype undergoing lateral undulation, using a traveling sinusoidal curvature wave over its length. Snapshots are taken in equal time intervals of 2 sec.

value, set as $P_m = 20.7$ kPa. Snapshots of a locomotion experiment of the soft snake with these parameters taken in 2 second intervals are displayed in Fig. 9. The robot traversed 18.4 ± 4 mm between each snapshot in this experiment, resulting in a net forward locomotion speed of 9.2 mm/sec on average. The gait algorithm is realized on an Arduino board using an external valve array.

B. Parallel Composition

A parallel composition of FEAs arranged around a hollow cylindrical core to achieve a soft rolling robot is displayed in Fig. 10.

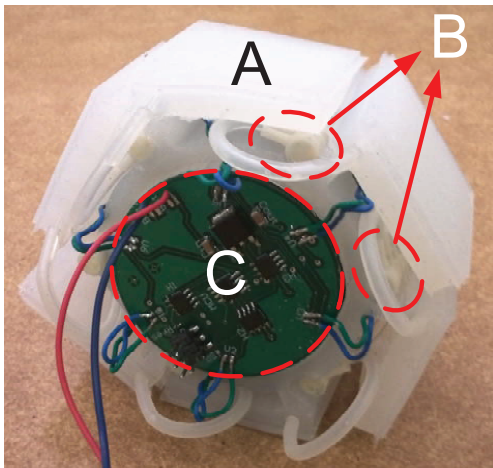


Fig. 10. Prototype of a rolling mobile robot, Flipper, made of six fluidic elastomer actuators (A) acting as flaps to propel the body forward. Embedded valves (B) under each FEA module drive the actuators. A custom PCB (C), designed to operate by 7.4 V input voltage (2 miniature LiPoly cells) and low power requirements computes the actuation sequence.

This robot is composed of six FEAs that act as flaps, bending out to push the body forward when actuated. It has a cylindrical opening at its center to place the pneumatic battery for on-board pressure generation, which was previously demonstrated in [2]. Developments to the prior work in this paper include an on-board custom PCB, which drives the robot by sequentially actuating each FEA in order, and embedded miniature 3-way latching valves driven by the PCB. It takes about 15 hours to build this robot.

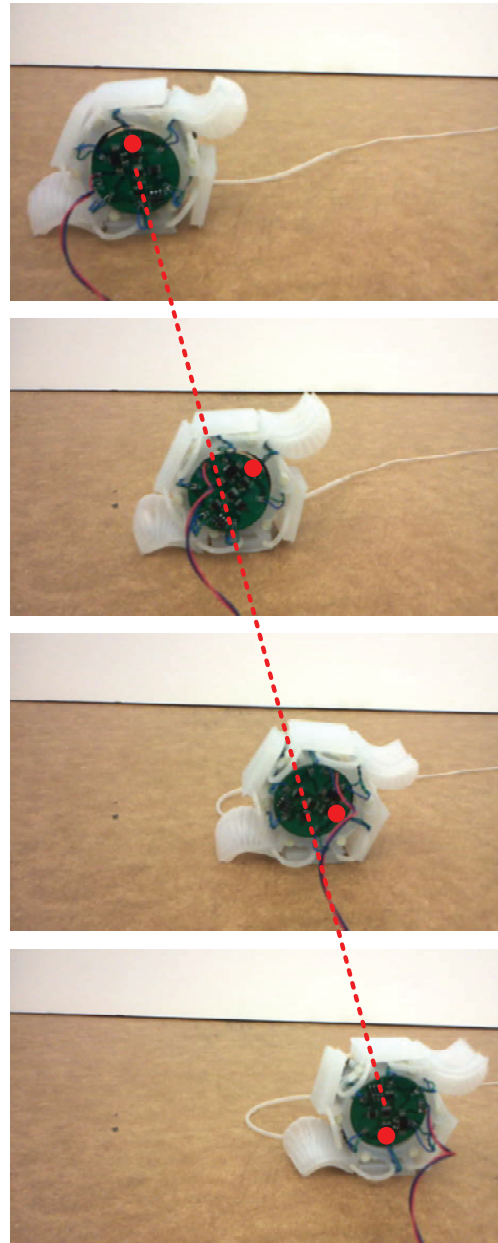


Fig. 11. Rolling locomotion experiment of Flipper. Three rolling steps are displayed from top to bottom. Actuated flaps that caused the motion are visible. Red dots are augmented to illustrate the orientation. The dashed red line shows the step-size repeatability. Snapshots are taken in equal time intervals of 10 sec.

Note that, given a long enough actuation period T_{on} for each segment, which depends on the input pressure,

this robot does not require sensors to keep rolling, as the actuation sequence will eventually reach the correct flap to start motion. Another improvement to previous work is the actuation of opposite segments (bottom and top) at the same time. This has two benefits. First, the number of control signals and driver circuits is cut by half, and second it enables the robot to push itself by the top flap as well if it is under an obstacle.

A sample rolling locomotion experiment is shown in Fig. 11 by snapshots taken every 10 seconds. For an input pressure of $P_{in} = 31$ kPa, the robot can take a rolling step in 6.25 sec on average and always less than 8 sec. For safety, we used an actuation period of $T_{on} = 10$ sec. When the pneumatic battery is placed on-board, the average rolling step increases to about 20 seconds. This is due to the additional weight of the battery and the time it takes to rebuild pressure after each step. The battery had a cut-off pressure value of 68.9 kPa, which was never reached during operation as the pressure generation in the battery was canceled by the pressure usage of the actuators [2]. This can also be improved by building a new generation pneumatic battery by traditional machining so that it can withstand larger pressure values. Each rolling step resulted in 52.3 mm of forward travel on average yielding an average speed of 5.23 mm/sec.

C. Hybrid Composition

Finally, an example hybrid configuration that is a combination of serial and parallel compositions is displayed in Fig. 1(A-C). This is a soft 1-D linear positioner made of 12 FEAs. It has $n_l = 6$ basis elements attached in parallel. Each of these elements is, in turn, made of two FEAs that bend in opposite directions, connected in series. Thus, the bending angle induced by one FEA is canceled by the other one, to achieve a linear motion. The displacement output of the positioner is equal to the displacement output of each finger, while the total force output is the sum of their individual contributions. It takes about 10 hours to build this mechanism.

Operation of this composition can be analyzed starting from the deformation of FEA modules. The bending angle θ_l of each half of a basis element is given as [2]

$$\theta_l = n \arctan \frac{l_c \varepsilon_x(\sigma_x)}{2h_c}, \quad (5)$$

where n is the number of channels in the actuator, l_c is the channel width, h_c is the channel thickness, and $\varepsilon_x(\sigma_x)$ defines the axial strain of the material as a function of the axial stress directly induced by the pressure input. This stress-strain relation is non-linear and described by a power function fit to experimental true stress and strain data. The total lateral deflection δ_l of the tip of each basis element becomes:

$$\delta_l = \frac{l_t}{\theta_l} (1 - \cos \theta_l), \quad (6)$$

where l_t is the total length of the element.

In turn, the bending moment M_b induced in each half is

$$M_b = P_{in} w_c h_c h_o, \quad (7)$$

for pressure input P , where w_c is the channel length, and h_o is the height offset (moment arm) of the average axial force generated by the pressure input. From this equation, the total lateral force F_l at the top layer of the linear positioner is written as:

$$F_l = 4n_l \frac{M_b}{l_t}. \quad (8)$$

With this analysis, we can predict the force and displacement characteristics of a completely soft linear motion platform, and adjust these values by tuning parameters for a given task.

IV. DISCUSSION

We presented a modular methodology of creating new soft robots that offer inherent safety and adaptability. These robots are based on pressure-operated actuation modules called fluidic elastomer actuators (FEAs). FEAs are fundamentally flat strips of elastomer that undergo bending deformation when pressurized. A number of these basic elements, when connected in different arrangements can accomplish increasingly complicated tasks as compared to traditional systems which might find those tasks difficult.

While they are less precise, these robots are robust in the presence of position errors, soft locomoters can traverse rough terrain, soft grippers can grasp objects of unknown or imprecisely specified geometries. Their compliance, in effect, can compensate for some of the challenges of current actuation and transmission technology.

We described and analyzed components of this soft robotic architecture, building up on our prior results. We presented a dynamic model of FEAs. The resulting theory was suitable for realistic control system design. We disclosed progress on the new pneumatic battery technology, which enables portable pressure generation with a chemomechanical process, similar to an electrical battery. Using better catalysts and an improved design, the battery was easier to tune for a given operation pressure, and achieved better repeatability. We overviewed sensors and computation technologies that are appropriate for the modularity in our soft robotic platforms, with examples.

Finally, we demonstrated main types of composition techniques to build soft robots of various functionalities. Instances of robots, resulting from each composition, are described with operation principles, algorithms and experimentally investigated.

There are many directions of soft robotics we pursue research on. Progress on developing custom miniature valves embedded in FEAs during fabrication, based on our prior work in [3], is important to achieve robots of large degrees of freedom. Reducing the size and increasing the pressure output of the pneumatic battery is another future work, also necessary for small mobile robots, such as the soft snake. Our main objective for this research is building a plug-and-play battery for pneumatic systems.

We are also working towards a soft manipulator arm. Future work on this area includes the development of forward and inverse kinematic models, embeddable soft sensors,

whole body manipulation, grasping methods, and obstacle negotiation.

REFERENCES

- [1] N. Correll, C. D. Onal, H. Liang, E. Schoenfeld, and D. Rus, "Soft autonomous materials - using active elasticity and embedded distributed computation," in *12th International Symposium on Experimental Robotics*, New Delhi, India, 2010.
- [2] C. D. Onal, X. Chen, G. M. Whitesides, and D. Rus, "Soft mobile robots with on-board chemical pressure generation," in *International Symposium on Robotics Research (ISRR)*, 2011.
- [3] A. Marchese, C. D. Onal, and D. Rus, "Soft robot actuators using energy-efficient valves controlled by electropermanent magnets," in *IEEE/RSJ International Conference on Intelligent Robots and Systems (IROS)*, 2011.
- [4] K. Wait, P. Jackson, and L. Smoot, "Self locomotion of a spherical rolling robot using a novel deformable pneumatic method," in *Robotics and Automation (ICRA), 2010 IEEE International Conference on*, may. 2010, pp. 3757–3762.
- [5] A. Albu-Schaffer, O. Eiberger, M. Grebenstein, S. Haddadin, C. Ott, T. Wimbock, S. Wolf, and G. Hirzinger, "Soft robotics," *IEEE Robotics & Automation Magazine*, vol. 15, pp. 20–30, Sep. 2008.
- [6] D. Trivedi, C. Rahn, W. Kier, and I. Walker, "Soft robotics: Biological inspiration, state of the art, and future research," *Advanced Bionics and Biomechanics*, vol. 5, no. 2, pp. 99–117, 2008.
- [7] H. Kazerooni, "Design and analysis of pneumatic force generators for mobile robotic systems," *IEEE/ASME Transactions on Mechatronics*, vol. 10, no. 4, pp. 411–418, 2005.
- [8] Y. Lianzhi, L. Yuesheng, H. Zhongying, and C. Jian, "Electropneumatic pressure servo-control for a miniature robot with rubber actuator," in *Digital Manufacturing and Automation (ICDMA), 2010 International Conference on*, vol. 1, 2010, pp. 631–634.
- [9] O. Ivlev, "Soft fluidic actuators of rotary type for safe physical human-machine interaction," in *IEEE 11th International Conference on Rehabilitation Robotics*, 2009.
- [10] M. Calisti, M. Giorelli, G. Levy, B. Mazzolai, B. Hochner, C. Laschi, and P. Dario, "An octopus-bioinspired solution to movement and manipulation for soft robots," *Bioinspiration & Biomimetics*, vol. 6, no. 3, p. 036002, 2011.
- [11] E. Kaniusas, H. Pfutzner, L. Mehnen, J. Kosel, G. Varoneckas, A. Alonderis, T. Meydan, M. Vizquez, M. Rohn, A. Merlo, and B. Marquardt, "Magnetoelastic skin curvature sensor for biomedical applications," in *IEEE Sensors*, 2004.
- [12] C. Majidi, R. Kramer, and R. J. Wood, "A non-differential elastomer curvature sensor for softer-than-skin electronics," *Smart Materials and Structures*, vol. 20, no. 10, p. 105017, 2011.
- [13] Y. Bahramzadeh and M. Shahinpoor, "Dynamic curvature sensing employing ionic-polymer-metal composite sensors," *Smart Materials and Structures*, vol. 20, no. 9, p. 094011, 2011.
- [14] J. K. Hopkins, B. W. Spranklin, and S. K. Gupta, "A survey of snake-inspired robot designs," *Bioinspiration & Biomimetics*, vol. 4, no. 2, p. 021001, 2009.
- [15] S. Hirose, *Biologically Inspired Robots: Snake-Like Locomotion and Manipulators*. Oxford University Press, 1993.
- [16] D. L. Hua, J. Nirodya, T. Scotta, and M. J. Shelleya, "The mechanics of slithering locomotion," *Proceedings of the National Academy of Sciences (PNAS)*, vol. 106, no. 25, pp. 10 081–10 085, 2009.
- [17] Z. V. Guo and L. Mahadevan, "Limbless undulatory propulsion on land," *Proceedings of the National Academy of Sciences (PNAS)*, vol. 105, no. 9, pp. 3179–3184, 2008.